Morphology of Symmetric ABC Triblock Copolymers in the Strong Segregation Limit

ARTICLE *in* MACROMOLECULES · JANUARY 1998

Impact Factor: 5.8 · DOI: 10.1021/ma971046o

2 AUTHORS, INCLUDING:

Glenn H Fredrickson
University of California, Santa Barbara

434 PUBLICATIONS **28,369** CITATIONS

Morphology of Symmetric ABC Triblock Copolymers in the Strong Segregation Limit

S. Phan* and G. H. Fredrickson

Chemical Engineering and Materials Departments, University of California, Santa Barbara, California 93106

Received July 15, 1997; Revised Manuscript Received October 22, 1997®

ABSTRACT: We investigate the equilibrium morphological properties of a symmetric ABC triblock copolymer in the strong segregation regime. Although a tricontinuous double diamond phase has been experimentally reported within a large region of the phase diagram, we find that neither gyroid nor double diamond cubic phases are stable relative to lamellae and cylinders in the asymptotic limit of strong segregation (SSL). However, this finding does not rule out stable equilibrium cubic phases at intermediate molecular weights or moderate temperatures. Moreover, in contrast to the experimental conclusions, the gyroid structure is shown to be marginally stable with respect to the double diamond structure in the SSL.

I. Introduction

One fascinating feature of block copolymers is their ability to self-assemble at sufficiently low temperature into a wide variety of ordered nanoscale morphologies whose characteristics can be easily controlled by changing the molecular weight, architecture, or composition. The simplest case, that of the AB diblock copolymer system, is now rather well understood, both from an experimental and from a theoretical point of view. Particularly due to recent advances that have allowed the unification of weak and strong-segregation theories,[1] the phase diagram of this system is now available for all chain compositions and throughout the entire temperature range. It can be summarized as follows: when the fraction of one component deviates from 1/2 (that is when the system becomes increasingly asymmetric), transitions occur to structures which possess more interfacial curvature. Thus, from a lamellar phase, the system goes through a hexagonal cylindrical phase to reach a body-centered cubic (bcc) spherical phase. Moreover, in the intermediate segregation regime (when $\chi N \sim 15$-60, where N is the chain length and χ the Flory interaction parameter between the two components), the so-called gyroid (G) phase is found to be stable between the lamellar and the cylindrical phases, which is in agreement with experiments.[2] Let us recall that the G phase corresponds to a structure where the minority component forms two continuous interpenetrating threefold-coordinated lattices in a matrix of the majority component (space group $Ia\bar{3}d$). The observation of this bicontinuous cubic phase [similar phases in low molecular weight surfactant systems are sometimes referred to as "plumbers' nightmare" (PN) phases] was for a long time associated with an ordered-bicontinuous-double-diamond (OBDD) structure that consists of two fourfold-coordinated lattices (space group $Pn\bar{3}m$).[3] The relative stability of G compared to OBDD in undiluted AB diblock copolymer melts is now well accepted.

The situation is less clear for ABC triblock copolymers, which are composed of three consecutive different blocks. First of all, the phase diagram is controlled by a larger number of parameters. In ABC triblock melts, there exist two independent segment compositions, e.g. f_A and f_B ($f_C = 1 - f_A - f_B$), and three Flory interaction parameters, χ_{AB}, χ_{BC}, and χ_{AC}. As a consequence, many fascinating new structures have turned up: for example, the cylinder-ring phase[4] is one of several nanophase morphologies discovered by Stadler and co-workers. Secondly, a cocontinuous PN phase appears to be stable throughout a *large* region of the phase diagram, in contrast to the case of AB diblock melts. Nevertheless, the nature of this PN phase remains unclear: early experiments reported the existence of an ordered-tricontinuous-double-diamond (OTDD) structure (space group $F\bar{4}3m$) in symmetric ABC triblock melts,[5] which is closely related to OBDD, but this identification preceded the OBDD structure being ruled out in favor of G in the AB diblock case.[2] Therefore, it seems possible that the experimentally observed PN structure might actually correspond to another tricontinuous phase, namely the "gyroid" phase in which threefold-coordinated lattices of A and C penetrate a B matrix (space group $I4_132$). In any case, from a technological point of view, ABC triblock copolymers offer a convenient route to cocontinuous nanostructured materials and could be used to formulate novel mesoporous solids, toughened plastics, or polymer membranes.

In the present paper, we theoretically investigate the relative stability of the OTDD and ($I4_132$) G phases at low temperatures (strong segregation limit) for a class of symmetric ABC triblock copolymers with equal A and C block lengths. This closely corresponds to the experimental situation described by Mogi *et al.*[5] with a poly(isoprene-*b*-styrene-*b*-2-vinylpyridine) system. Several theoretical approaches are possible. In the weak-segregation limit, Leibler has developed a mean-field theory for diblock systems[6] that can be extended to ABC systems[7] and PN phases.[8] In the intermediate segregation regime, the self-consistent field theory of Matsen and Schick,[1] based on the work of Helfand[9] and Hong and Noolandi,[10] is extremely powerful, yet numerically intensive. In the strong-segregation limit (SSL), approaches developed by Ohta and Kawasaki,[11] Likhtman and Semenov,[13] or Olmsted and Milner[14] can be used.

® Abstract published in *Advance ACS Abstracts,* December 15, 1997.

S0024-9297(97)01046-2 CCC: $15.00
Published on Web 01/13/1998

The former approach, that of Ohta and Kawasaki, has already been applied to ABC triblock systems,[15,16] and has demonstrated a possible stability of OTDD for certain values of a parameter that could not be optimized by free energy minimization.[15] Our present aim is to reanalyze this possibility within the framework of the two more recent SSL theoretical approaches[13,14] and to contrast OTDD stability with that of G.

II. Theory and Results

We adopt a symmetrical model of ABC triblock copolymers. The A, B, and C monomers are supposed to have the same size and shape, with volume Ω/N (where Ω is the total volume of a chain) and statistical segment length b. As a consequence $f_A = f_C$ in our study. Moreover, we will consider the case of such a strong incompatibility between components A and C ($\chi_{AC} \gg \chi_{AB}$ and χ_{BC}) that no A−C interfaces are present.

The low-temperature (SSL) self-assembly of block copolymers can be understood as the result of a competition between interfacial tension, which tends to minimize the interfacial area separating regions containing different blocks, and the stretching free energy which arises because chains must extend away from the interfaces in order to fill the microdomains at uniform monomer density. These two terms have distinct scaling with R, the length scale (microdomain period) of a given structure. By minimizing the total free energy per chain, f, with respect to R, one obtains the equilibrium length scale R_{eq} and the equilibrium free energy f_{eq} of the structure. The overall phase diagram is generated by comparing f_{eq} for various assumed structures.

We now consider the free energy of our model triblock copolymer melt in an elementary cell (to be defined below). In the strong segregation regime, it can be written as[17]

$$F = F_{int} + F_{el} \tag{1}$$

where F_{int} is the interfacial term and F_{el} is the elastic part. The former has two contributions, one from the A−B interface and the other from the B−C interface:

$$F_{int} = \gamma_{AB} S_{AB} + \gamma_{BC} S_{BC} \tag{2}$$

where $\gamma_{ij} \sim k_B T \chi_{ij}^{1/2} b^{-2}$ is the interfacial tension between i and j (i and $j \equiv$ A or B), k_B is Boltzmann's constant, T is the temperature, and S_{ij} is the area of the i−j interface contained in the cell.[12]

The elastic part of the free energy contains three contributions:

$$F_{el} = F_A + F_B + F_C \tag{3}$$

The end-block terms F_A and F_C can be treated in the usual way: we allow the free ends of the chains to lie at any distance from the dividing surface. Because the chemical potential is quadratic in the distance from the interface,[13,14] regardless of the chain end location, the elastic energy can be conveniently summed up by an integral over the appropriate domain. Thus, if $\mathbf{r}$ is an interior point of the A domain and $z(\mathbf{r})$ is the distance of that point from the A−B interface (see below), the elastic energy of the A microdomain is

$$F_A = \frac{3\pi^2}{8} \frac{k_B T}{f_A^2 l^2 \Omega} \int_{[A]} z^2(\mathbf{r})\, d\mathbf{r} \tag{4}$$

where $l^2 = Nb^2$ and $\int_{[A]} d\mathbf{r}$ denotes an integration over the A domain.[18] A similar expression for F_C can be immediately written down.

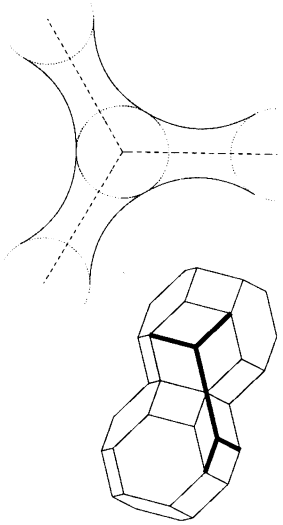

Figure 1. Lower figure: the ($I4_132$) gyroid structure is composed of two interpenetrating lattices of A and C. This can be generated by continuously packing Wigner−Seitz cells of the body-centered-cubic Bravais lattice, each of them containing two threefold knots of A and C on two opposite hexagonal sides. Above the figure, we depict the interface shape between a minority component and the matrix B. These structures are constructed by assembling paraboloids of revolution and spheres. A similar process is used to represent the OTDD structure.

In the present work, we suppose that the A and C domains have a well-defined shape for each structure, which only depends on one parameter (related to the length scale R of the structure). For the cases of lamellar, hexagonal, and spherical phases, this shape is given, respectively, by a planar layer, a cylinder, or a sphere. However, as pointed out by Matsen *et al.*, there is no reason to restrict consideration to (or even to expect) constant mean curvature (CMC) surfaces in the strong segregation limit.[19,20] Thus, we choose not to make use of minimal surfaces in treating the OTDD and G phases and instead construct approximate representations of these PN structures as illustrated in Figure 1. In particular, on each knot of a sublattice, the A (or C) domain is delimited by a sphere that continuously connects, at the half-tetrahedral angle (for OTDD) or $\pi/3$ (for G), to a paraboloid of revolution that constitutes each joining segment of the lattice (see Figure 1).[21] For a given sphere radius, the geometry of the A−B or B−C interfaces is uniquely determined and resembles a CMC surface when f_A (or f_C) ~0.15, a situation in which we might anticipate stability of a PN structure.

The middle B block is different from the A and C end-blocks because its end monomers (at the A−B and B−C junctions) are constrained (in the SSL) to lie on the A−B or B−C interfaces. Moreover, the equal time constraint[22] which led to eq 4 is no longer applicable. Indeed, the end-blocks in the present ABC triblock context can be likened (in a one-dimensional situation) to the parabolic brush of Milner *et al.*,[22] while the B

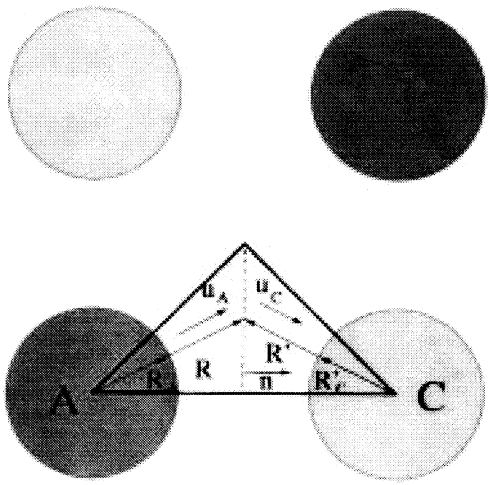

Figure 2. Tetragonal structure of cylindrical A and C domains. An elementary cell is drawn. The dashed and thin lines inside the cell represent, respectively, the separating surface and a straight path approximation to a chain trajectory.

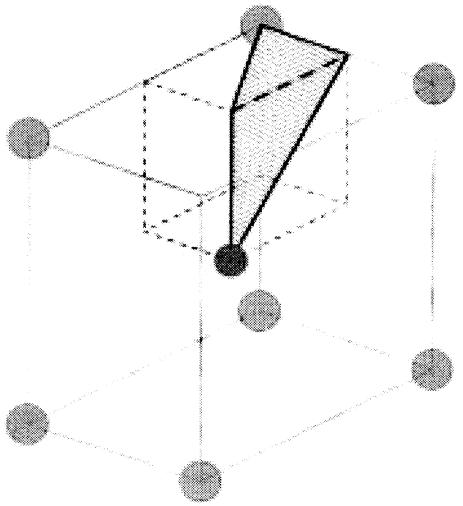

Figure 3. Body-centered-cubic structure of spherical domains. One of the two different elementary cells is depicted (the other is symmetrical).

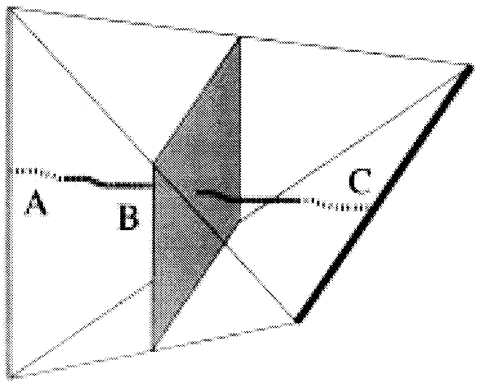

Figure 4. An elementary cell for the PN phases. Its shape depends on the relative orientation of A and C segments. While there is only one elementary cell for OTDD, two different kinds of cells are needed to construct the gyroid structure. The separating plane divides the cell in two identical parts.

center-blocks resemble the step brush of Alexander.[23] One might anticipate that the "bridge effect" arising from the tethering of both ends of the B blocks is responsible for the experimentally-observed enhancement of PN phase stability in ABC triblocks relative to AB diblocks.

Next, we specify our choice of elementary cells in the triblock case. For a given structure, the elementary cells are the smallest subunits that can be packed together to compose the structure while still respecting its overall symmetry. More than one type of elementary cell may be required to describe a given structure, as for instance in the case of the CsCl spherical phase and the G phase (see below). Note that individual chains are entirely contained within a cell and are not cut by the cell boundaries. Moreover, since the end-blocks of the chains play a symmetrical role, each elementary cell is necessarily symmetrical. A plane, which we refer to as the *separating surface* of the cell, divides each cell into two identical parts containing, respectively, only A and B or B and C monomers. Some examples are given in Figures 2–4.

Our remaining task is to estimate the elastic part of the free energy contributed by the center B-block chains in an elementary cell, taking account of the incompressibility constraint. To fulfill this constraint, we suppose that in each of the half-elementary cells, chains follow a *straight path approximation*. The elastic energy along the path in the B domain will be computed by using the "wedge method" of Milner *et al.*[14] Each B block belongs to two wedges that are connected at the separating surface and successively oriented by $\mathbf{u_A}$ and $\mathbf{u_C}$, two unit vectors. It is possible to define a flux of B monomers going through the separating surface, but as the direction of path is generally discontinuous at this point, we prefer to use the notion of a surface density of chains σ. If dS is the corresponding area element of the separating surface, σdS is then the number of chains contained in the wedges:

$$\sigma = \frac{1}{f_B \Omega}\left[\int_{R_A}^{R} dz\, a(z,R)\, \mathbf{u_A}\cdot\mathbf{n} + \int_{R_C}^{R'} dz\, a(z,R')\, \mathbf{u_C}\cdot\mathbf{n}\right] \tag{5}$$

where R_A and R represent distances between the end of the chain (on the A side) and, respectively, the corresponding junction between A–B domains and the corresponding point of the separating surface, within the straight path approximation (see for instance Figure 2). A similar definition for R'_C and R' is used. $\mathbf{u_A}$ and $\mathbf{u_C}$ are two unit vectors following the path of a given chain, $\mathbf{n}$ is the normal vector to the separating surface (oriented from A to C), and

$$\begin{aligned} a(z,R) &= 1 && \text{lamellae} \\ a(z,R) &= z/R && \text{cylinders} \\ a(z,R) &= (z/R)^2 && \text{spheres} \\ a(z,R) &= z/R\,(2 - z/R) && \text{PN} \end{aligned} \tag{6}$$

are the relative areas as a function of the relative height z/R along the center normal in the wedges representing the different structures.[14]

Following ref 24, one can evaluate the stretching energy of one B branch of a given wedge by summing along the path over the local rate of deformation $3[k_B T \partial z/\partial n]/2b^2$. Taking into account all contributions

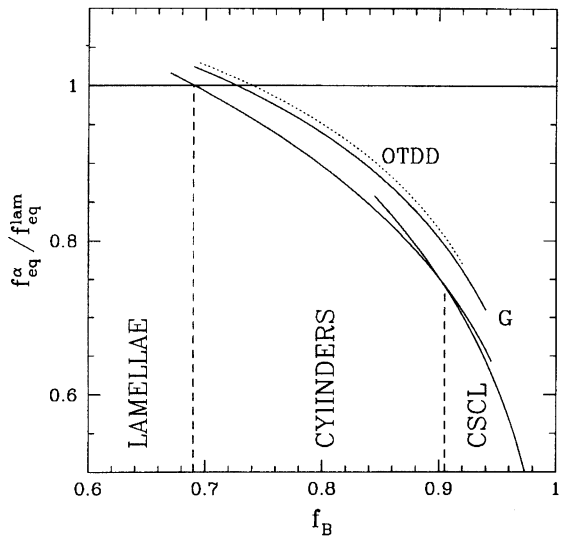

Figure 5. Equilibrium free energy for lamellar, cylindrical (tetragonal), spherical (CsCl), OTDD, and gyroid structures.

in an elementary cell, one obtains:

$$F_B = \int dS\,\sigma^2 \frac{3k_BT}{2b^2}\frac{\Omega}{N}\left[\int_{R_A}^{R} dz \frac{1}{a(z,R)\,\mathbf{u_A}\cdot\mathbf{n}} + \int_{R_C}^{R} dz \frac{1}{a(z,R)\,\mathbf{u_C}\cdot\mathbf{n}}\right] \quad (7)$$

Proceeding the same way for all the structures, the free energy per chain can finally be written as:

$$f = \frac{F}{\int dS\,\sigma} = f_{el}R^2 + \frac{f_{int}}{R} \quad (8)$$

where $\{f_{el}, f_{int}\}$ are two constant coefficients that depend on the structure. When minimized with respect to R, the equilibrium free energy per chain is:

$$f_{eq} = \frac{3}{2^{2/3}} f_{el}^{1/3} f_{int}^{2/3} \quad (9)$$

Note that in the gyroid structure, a segment of one minority component (this is the portion between two knots of the corresponding threefold sublattice) belongs to 10 elementary cells similar to that of Figure 4, but of two different kinds. One of the groups contains eight equivalent cells, while the other contains only two identical cells. We take account of this in the calculations and perform an average over the different cells. A similar procedure is required in the case of the CsCl and FCC (face-centered-cubic) spherical structures.

In Figures 5 and 6, we plot the equilibrium free energy f^{α}_{eq} for various structures α and compare it to the lamellar free energy. For $0 \le f_B \le 0.69$, we show that the triblock system exhibits a lamellar state at equilibrium in the SSL. For $0.69 \le f_B \le 0.905$, we found that the tetragonal cylindrical structure is the most stable. For $0.905 \le f_B$, the body-centered-cubic spherical phase (CsCl) seems to be the lowest in free energy. Neither of the PN phases (OTDD or G) is found to be stable. We may conclude that, in the strong segregation regime, the "bridge effect" present in the triblock system is not strong enough to induce a new behavior when compared to the diblock case. Nevertheless, in contrast to previous experimental conclusions,[5] we have found

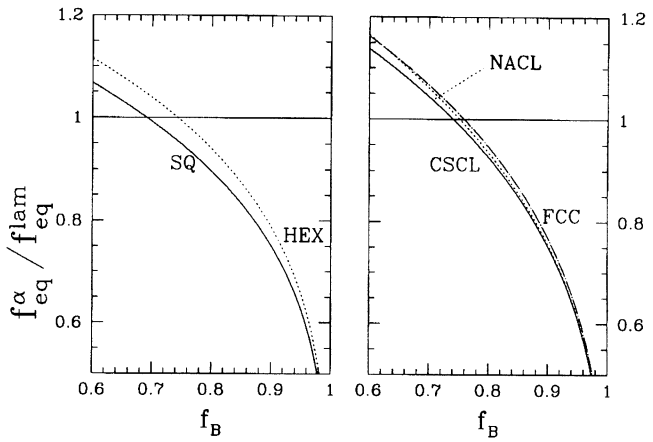

Figure 6. Equilibrium free energy for various cylindrical (left) and spherical (right) structures.

that the G structure is marginally stable with respect to the OTDD structure. By analogy with the situation for AB diblocks, it seems likely that the G structure may prove to be stable in the intermediate segregation regime, in which case the experimental postulate of OTDD should be reexamined.

As in earlier studies,[15,16] we found that the cylindrical domains constitute a square lattice for triblock copolymers (see the left side of Figure 6), while an hexagonal lattice is observed in the diblock case. Indeed the first situation is more favorable, because as explained in ref 15 less frustration occurs for the triblock chains in that case. On the right side of Figure 6, we also have examined several kinds of spherical domains. Our results are similar to those of ref 15. The CsCl type structure yields the lowest equilibrium free energy for the whole range of f_B, in contrast to our calculations for the NaCl and FCC structures.

Acknowledgment. S.P. wishes to thank B. Campbell for useful discussions. This work was supported by the National Science Foundation under Award No. DMR95-05599.

References and Notes

(1) Matsen, M. W.; Bates F. S. *J. Chem. Phys.* **1997**, *106*, 2436. Matsen, M. W.; Schick, M. *Phys. Rev. Lett.* **1994**, *72*, 2660.
(2) Hadjuk, D. A.; Harper, P. E.; Gruner, S. M.; Honeker, C. C.; Kim, G.; Thomas, E. L.; Fetters, L. J. *Macromolecules* **1994**, *27*, 4063. Schulz, M. F.; Bates F. S.; Almdal, K.; Mortensen, K. *Phys. Rev. Lett.* **1994**, *73*, 86.
(3) Thomas, E. L.; Alward, D. B.; Kinning, D. J.; Martin, D. C. Handlin, D. L.; Fetters, L. J. *Macromolecules* **1986**, *19*, 2197. Hadjuk, D. A.; Harper, P. E.; Gruner, S. M.; Honeker, C. C.; Thomas, E. L.; Fetters, L. J. *Macromolecules* **1995**, *28*, 2570.
(4) Auschra, C.; Stadler, R. *Macromolecules* **1993**, *26*, 2171. Beckmann, J.; Auschra, C.; Stadler, R. *Macromol. Rapid Commun.* **1994**, *15*, 67.
(5) Mogi, Y.; Kotsuji, H.; Kaneko, Y.; Mori, K.; Matsushita, Y.; Noda, I. *Macromolecules* **1992**, *25*, 5408. Mogi, Y.; Mori, K.; Matsushita, Y.; Noda, I. *Macromolecules* **1992**, *25*, 5412. Matsushita, Y.; Tamura, M.; Noda, I. *Macromolecules* **1994**, *27*, 3680. Mogi, Y.; Nomura, M.; Kotsuji, H.; Ohnishi, K.; Matsushita, Y.; Noda, I. *Macromolecules* **1994**, *27*, 6755.
(6) Leibler, L. *Macromolecules* **1980**, *13*, 1602.
(7) Werner, A.; Fredrickson, G. H. *J. Polym. Sci.: Part B: Polym. Phys.* **1997**, *35*, 849.
(8) Milner, S. T.; Olmsted, P. D. *J. Phys II Fr.* **1997**, *7*, 249.
(9) Helfand, E. *J. Chem. Phys.* **1975**, *62*, 999.
(10) Hong, K. M.; Noolandi, J. *Macromolecules* **1981**, *14*, 727.
(11) Ohta, T.; Kawazaki, K. *Macromolecules* **1986**, *19*, 2621.
(12) Here $S_{AB} = S_{BC}$, as a consequence the interfacial free energy F_{int} depends only on the sum $\gamma_{AB} + \gamma_{BC}$. Thus, when later

considering the relative total free energy between the different structures, the dependence on interfacial tensions will vanish.
(13) Likhtman A. E.; Semenov, A. N. *Macromolecules* **1994**, *27*, 3103.
(14) Olmsted P. D.; Milner, S. T. *Phys. Rev. Lett.* **1994**, *72*, 936; erratum *Phys. Rev. Lett.* **1995**, *74*, 829. Xi H.; Milner S. T. *Macromolecules* **1996**, *29*, 2404.
(15) Nakazawa, H.; Ohta, T. *Macromolecules* **1993**, *26*, 5503.
(16) Zheng, W.; Wang Z. G. *Macromolecules* **1995**, *28*, 7215.
(17) Semenov, A. N. *Macromolecules* **1985**, *61*, 733.
(18) We note that eq 4 is not appropriate in situations (e.g. convex layers) where "dead zones" are present.
(19) Matsen, M. W.; Bates F. S. *Macromolecules* **1996**, *29*, 1091.
(20) A proper treatment would consist in determining the interfacial shape self-consistently.
(21) We have recovered results of refs 13 and 14 for diblock copolymer system, using these shapes for the minority component domains in the G and the OBDD structures.
(22) Milner, S. T.; Witten, T. A.; Cates, M. E. *Macromolecules* **1988**, *21*, 2610.
(23) Alexander, S. *J. Phys. (Les Ulis, Fr.)* **1977**, *38*, 983.
(24) Fredrickson, G. H. *Macromolecules* **1991**, *24*, 3456.

MA971046O